ACS Chemical Neuroscience

Research Article

pubs.acs.org/chemneuro

Toxicity Inhibitors Protect Lipid Membranes from Disruption by Aβ42

Ravit Malishev,[†] Sukhendu Nandi,[†] Sofiya Kolusheva,[‡] Yael Levi-Kalisman,[†] Frank-Gerrit Klärner,[§] Thomas Schrader,[§] Gal Bitan,[*,∥] and Raz Jelinek[*,†,‡]

[†]Department of Chemistry, Ben Gurion University of the Negev, Beer Sheva 84105, Israel

[‡]Ilse Katz Institute for Nanotechnology, Ben Gurion University of the Negev, Beer Sheva 84105, Israel

[§]Institute of Organic Chemistry, University of Duisburg-Essen, Essen 45117, Germany

[∥]Department of Neurology, David Geffen School of Medicine, Brain Research Institute, and Molecular Biology Institute, University of California at Los Angeles, Los Angeles, California 90095, United States

Supporting Information

ABSTRACT: Although the precise molecular factors linking amyloid β-protein (Aβ) to Alzheimer's disease (AD) have not been deciphered, interaction of Aβ with cellular membranes has an important role in the disease. However, most therapeutic strategies targeting Aβ have focused on interfering with Aβ self-assembly rather than with its membrane interactions. Here, we studied the impact of three toxicity inhibitors on membrane interactions of Aβ42, the longer form of Aβ, which is associated most strongly with AD. The inhibitors included the four-residue C-terminal fragment Aβ(39−42), the polyphenol (−)-epigallocatechin-3-gallate (EGCG), and the lysine-specific molecular tweezer, CLR01, all of which previously were shown to disrupt different steps in Aβ42 self-assembly. Biophysical experiments revealed that incubation of Aβ42 with each of the three modulators affected membrane interactions in a distinct manner. Interestingly, EGCG and CLR01 were found to have significant interaction with membranes themselves. However, membrane bilayer disruption was reduced when the compounds were preincubated with Aβ42, suggesting that binding of the assembly modulators to the peptide attenuated their membrane interactions. Importantly, our study reveals that even though the three tested compounds affect Aβ42 assembly differently, membrane interactions were significantly inhibited upon incubation of each compound with Aβ42, suggesting that preventing the interaction of Aβ42 with the membrane contributes substantially to inhibition of its toxicity by each compound. The data suggest that interference with membrane interactions is an important factor for Aβ42 toxicity inhibitors and should be taken into account in potential therapeutic strategies, in addition to disruption or remodeling of amyloid assembly.

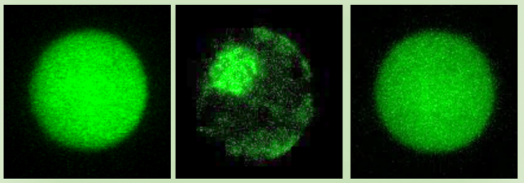

Effects of Aβ42 inhibitors on membrane interactions

KEYWORDS: *Molecular tweezer, membrane interactions, amyloid β-protein (Aβ), polyphenols, fibril inhibitors*

The transformation of soluble proteins into toxic oligomers and amyloid fibrils is a key pathologic process in devastating medical disorders, including Alzheimer's disease (AD), Parkinson's disease, and type-II diabetes.[1,2] Though the presence of fibrillar aggregates appears to be a universal phenomenon in amyloid diseases, the relationship between amyloid formation, disease progression, and pathogenicity remains unclear. Amyloid plaques, in which the main component is the amyloid β-protein (Aβ), particularly its longer form, Aβ42, are a pathologic hallmark of AD. Aβ oligomers, which form as intermediates in the plaque-formation process and are considered the proximal neurotoxins in AD, have been reported to cause membrane leakage, either through nonspecific pore formation or via other mechanisms.[3−5] A two-step mechanism for Aβ42−membrane interactions has been recently reported.[6] Accordingly, understanding the mechanistic aspects of Aβ42 interactions with cellular membranes has been the focus of intensive research.[7−10]

Diseases associated with protein misfolding and aggregation, including AD, are currently incurable. Therefore, extensive research effort has been directed at developing inhibitors and modulators of protein aggregation and exploring their therapeutic potential. Notably, however, despite strong evidence for involvement of lipid and membrane interactions of misfolded proteins in the cytotoxicity of amyloidogenic proteins,[11,12] development of therapeutic drugs targeting protein misfolding and aggregation largely has neglected this aspect of the pathologic mechanism and focused almost exclusively on substances that interfere with the self-assembly processes of amyloid proteins, such as Aβ42.

Numerous molecules have been evaluated for their effect on Aβ self-assembly and toxicity.[13−16] Peptide fragments compris-

Received: July 24, 2015
Accepted: August 28, 2015
Published: August 28, 2015

DOI: 10.1021/acschemneuro.5b00200
ACS Chem. Neurosci. 2015, 6, 1860−1869

ing discrete short sequences within Aβ42 have been shown to reduce cytotoxicity in cell culture and in vivo, presumably through binding to Aβ42 at early aggregation stages, thereby inhibiting formation of the toxic oligomers.[17,18] Polyphenols, such as resveratrol (found in red grape skin and seeds)[19,20] and (−)-epigallocatechin-3-gallate (EGCG, a component of green tea),[21,22] have been among the most widely studied inhibitors of cytotoxicity and fibril formation of amyloid proteins. These molecules have attracted much attention because they are nutraceuticals; they exist in different food sources and therefore are considered bioavailable and safe. Another attractive feature is that many of them also have antioxidant and anti-inflammatory activities.[23,24] EGCG, in particular, is a broad-spectrum inhibitor, previously shown to interfere in the Aβ42 fibrillation process at different stages, blocking toxic oligomer assembly,[22,25,26] and inducing fibril disassembly.[27,28] Amyloid inhibitory effects of small compounds derived from natural products have also been recently reported.[29]

Using a different approach, recent studies have identified a synthetic lysine-binding "molecular tweezer" called CLR01 as a powerful modulator of the self-assembly and a general inhibitor of the toxic effect of amyloid proteins, including Aβ42.[30,31] The mechanism of action of CLR01 is reversible binding to exposed lysine residues, which disrupts electrostatic and hydrophobic interactions involving lysines and leads to remodeling of the assembly process into formation of nontoxic and non-amyloidogenic structures that can be effectively degraded by the natural clearance mechanisms. Because the binding is highly labile and occurs with micromolar affinity and because in misfolded proteins lysines tend to be more exposed to the solvent than in typical globular proteins,[32] at the concentrations needed for inhibition, CLR01 does not interfere with normal protein structure or function.[31,33]

Here, we specifically address the participation of membranes in amyloid toxicity inhibition through investigating the effect of three modulators, Aβ(39−42), EGCG, and CLR01, on membrane interactions of Aβ42. These three inhibitors were chosen because they represent a variety of features some of which overlap and some that are unique to each compound (Table 1). Different than most assembly modulation studies reported to date, the focus of our study was on the ternary interactions among Aβ42, the assembly modulators, and membrane lipid bilayers. As such, our work illuminates a rarely studied angle of assembly modulators' activity, their effect on membrane interactions of Aβ. The data reveal that the interactions between Aβ42 and each assembly modulator effectively "shield" the membrane, not only blocking membrane interactions of Aβ42 but also, surprisingly, inhibiting bilayer disruption by the assembly modulators themselves.

Table 1. Details of the Assembly Modulators Studied

compound	EGCG	Aβ(39−42)	CLR01
type	small molecule	peptide	small molecule
specificity[a]	nonspecific	Aβ42	nonspecific
binds monomers	no	no	yes
binds oligomers	yes	yes	yes
specific binding site	no	mainly N-terminal region	Lys16 > Lys28 > Arg5

[a]Specificity refers to whether the compound binds one particular target or multiple targets, as well as targeting particular assembly states, monomers, oligomers, or fibrils.[22,30,34]

RESULTS AND DISCUSSION

Figure 1 shows the assembly modulators studied here and their putative effects on the Aβ42 assembly process. We selected

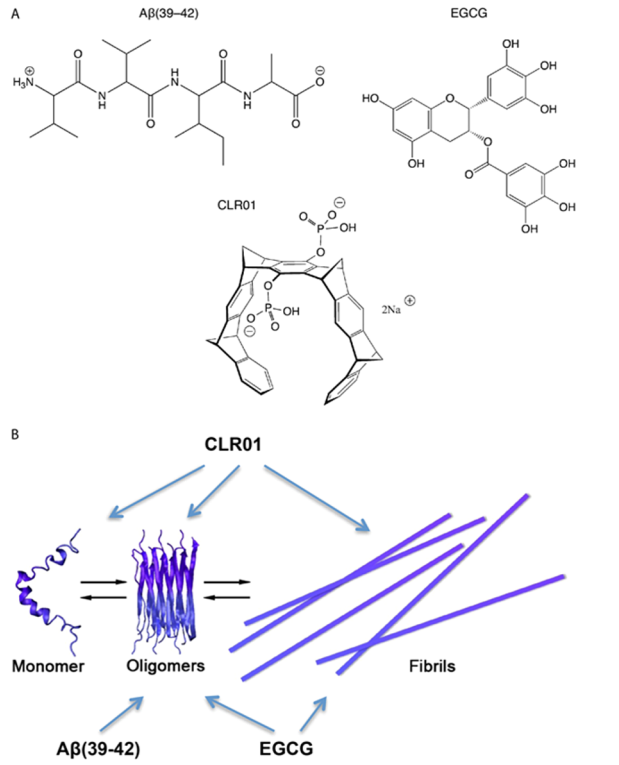

Figure 1. Assembly modulators studied and their putative activity. (A) The molecules investigated in this study: Aβ(39−42), EGCG, and CLR01. (B) Stages of Aβ42 fibrillation putatively modulated by compounds **1**−**3**.

these modulators because they belong to distinct molecular classes and they remodel Aβ42 using different mechanisms. Specifically, Aβ(39−42) (Figure 1A) comprises the four-residue C-terminal sequence of Aβ42 (Val-Val-Ile-Ala), which was shown to reduce Aβ42 neurotoxicity by remodeling its oligomerization but did not affect Aβ42 fibrillation.[18,34−36] EGCG is a polyphenol extracted from green tea known to bind Aβ oligomers, modify them covalently,[37] and inhibit their toxicity.[22,38] CLR01 is a molecular tweezer that binds Aβ monomers and oligomers noncovalently, thereby remodeling Aβ42 assembly and inhibiting its toxicity.[30,39,40] CLR01 also can disaggregate preformed Aβ fibrils, albeit with much slower kinetics than EGCG. Both EGCG and CLR01 are broad-spectrum assembly modulators that have been shown to be effective inhibitors of the toxicity of multiple amyloidogenic proteins,[38,41] whereas Aβ(39−42) inhibits Aβ42 selectively.[34,35]

Figure 1B summarizes the putative stages of the Aβ42 assembly process affected by each modulator.[34,35,39,42] It should be emphasized, however, that although the inhibition mechanisms depicted in Figure 1B are based on experimental analyses, the effects of the modulators in the presence of membranes and the interplay between assembly modulation and membrane interactions have not been addressed previously.

We compared first the fibrillation kinetics of Aβ42 modulator mixtures in buffer alone and in the presence of DMPC/DMPG vesicles. This vesicle composition has been employed widely as

DOI: 10.1021/acschemneuro.5b00200
ACS Chem. Neurosci. 2015, 6, 1860−1869

a mimetic of cellular membranes.[43,44] The kinetics of β-sheet formation was monitored using the thioflavin-T (ThT) fluorescence assay (Figure 2). ThT is a commonly used dye

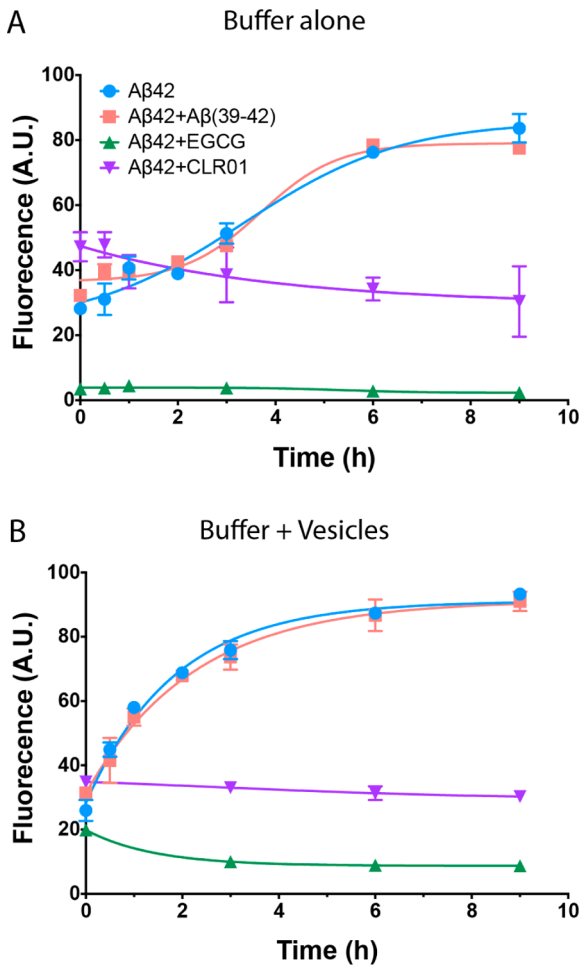

Figure 2. Fibrillation kinetics of Aβ42. ThT fluorescence was recorded in the absence (A) or presence (B) of DMPC/DMPG vesicles. The data are presented as mean ± SEM of two to four reactions with 10 readings of each sample at every time point.

exhibiting enhanced fluorescence upon binding to β-sheets in amyloid fibrils.[45,46] Importantly, ThT is not suitable for measurement of β-sheet formation and aggregation in the presence of some compounds, for example, curcumin, quercetin, and resveratrol, which have significant absorbance in the 440−482 nm range used for ThT excitation and emission.[47] However, none of the compounds that we used absorb in this range,[48,49] and therefore the ThT assay is suitable for measuring the formation of β-sheet-rich fibrils in the presence of these assembly modulators.

Figure 2 shows different fibrillation kinetics of Aβ42 in the absence or presence of DMPC/DMPG vesicles. In the absence of vesicles, a lag phase of ∼2 h was observed followed by an increase in fluorescence up to 6 h, at which point the fluorescence signal plateaued (Figure 2A). In contrast, in the vesicle-containing solution, the ThT fluorescence increased rapidly already within the first hour of incubation with no apparent lag phase (Figure 2B), suggesting that the presence of a membrane-like environment accelerated Aβ42 fibril nucleation, as reported previously.[50]

The assembly modulators had distinct effects on the fibrillation kinetics (Figure 2). The ThT fluorescence curves corresponding to the Aβ42/Aβ(39−42) mixture, both in buffer and in vesicle solutions, were almost identical to those of Aβ42 alone, in agreement with a previous report that Aβ(39−42) did not significantly affect the extent or kinetics of Aβ42 fibril formation.[34] In contrast, no increase in ThT fluorescence was observed in the presence of either EGCG or CLR01. In fact, in the presence of EGCG in buffer alone the initial fluorescence was substantially lower than in any of the other cases (Figure 2A). These data are in agreement with a previous report indicating that in addition to preventing Aβ fibril formation, EGCG competes with ThT binding to Aβ,[37] presumably leading to the apparent low fluorescence. In the presence of the lipid vesicles, the initial ThT fluorescence of the Aβ42/EGCG mixture was similar to that of the other reactions and then decreased gradually over time (Figure 2B), suggesting that initially the vesicles might shield, at least partially, the binding sites on Aβ from EGCG but not from ThT.

A lack of increase in ThT fluorescence intensity was observed also in the presence of CLR01 (Figure 2), which is not known to affect ThT binding to Aβ. Therefore, these data likely point simply to inhibition of β-sheet formation of Aβ42 by CLR01 regardless of the presence of the vesicles. Overall, the ThT fluorescence data suggest that the three modulators behave similarly in the presence of lipid vesicles to the way they behave in simple buffer solutions; namely, Aβ(39−42) does not affect fibril formation,[34] CLR01 prevents Aβ42 fibrillogenesis, whereas conclusions regarding the effect of EGCG on fibrillogenesis cannot be made due to its competition with ThT.[39]

Cryo-TEM analysis (Figure 3) corroborated the ThT data and provided a visual depiction of the effect of the modulators on Aβ42 in the presence of lipid vesicles. TEM examination of Aβ42 in the presence of each modulator in simple buffers has been reported previously[30,34,51] and therefore is not shown

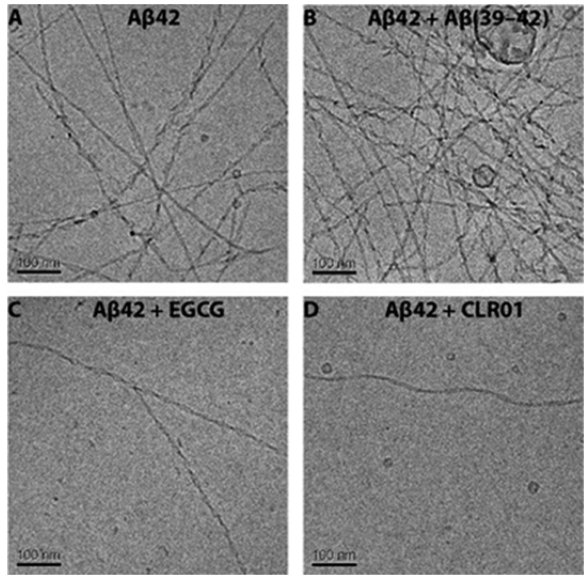

Figure 3. Aβ42 fibril morphology in the presence of membrane mimetics. Cryo-TEM images of Aβ42 samples after 12 h incubation with DMPC/DMPG vesicles. (A) Aβ42; (B) Aβ42 co-incubated with Aβ(39−42); (C) Aβ42 co-incubated with EGCG; (D) Aβ42 co-incubated with CLR01.

DOI: 10.1021/acschemneuro.5b00200
ACS Chem. Neurosci. 2015, 6, 1860−1869

here. Aβ42 alone or in the presence of Aβ(39−42) (as well as in the presence of DMPC/DMPG vesicles) formed abundant fibrils (Figure 3A,B), whereas when co-incubated with EGCG or CLR01 only scarce fibrils were observed (Figure 3C,D). Together, the ThT (Figure 2) and microscopy (Figure 3) experiments indicate that the effects of the three assembly modulators on Aβ42 fibrillation in the presence of lipid vesicles are similar to their effects in the absence of membranes.

To gain further insight into the impact of the ternary interactions among Aβ42, lipid vesicles, and assembly modulators on the changes in the secondary structure of Aβ42 during its self-assembly, we used CD spectroscopy (Figure 4). The CD spectra of Aβ42 in buffer alone showed a

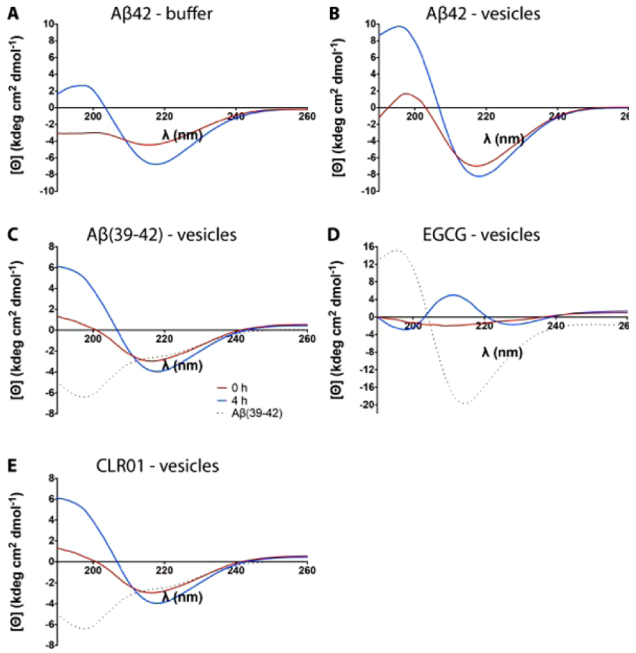

Figure 4. Aβ42 secondary structure. Time-dependent secondary structure change of Aβ42 monitored by CD spectroscopy in the absence (A) or presence (B−E) of vesicles and toxicity inhibitors. (A, B) Aβ42; (C) Aβ42 + Aβ(39−42); (D) Aβ42 + EGCG; (E) Aβ42 + CLR01. The red spectra were recorded at time = 0, while the blue spectra were taken after 4 h incubation. The spectra of the buffer and modulators were subtracted from each presented spectrum. Modulator spectra are presented as dotted lines for reference. Note that the *y*-axis scale is different for each modulator.

change from an initial mixture of statistical coil and β-sheet to a predominantly β-sheet conformation, reflected in spectral maxima at 195−198 nm and minima at 217−218 nm (Figure 4A).[52] Consistent with previous studies,[53] the presence of the lipid vesicles promoted β-sheet formation of Aβ42, giving rise particularly to increased intensity of the maxima at 195−198 nm (Figure 4B).

The three inhibitors had distinct effects on the folding of Aβ42 in the presence of vesicles (Figure 4C−E). Aβ(39−42) appeared not to disrupt β-sheet formation, although signal intensity was reduced by the peptide fragment (Figure 4C). Both EGCG and CLR01, however, significantly disrupted the β-sheet conformation of Aβ42. In the case of EGCG addition, the initial spectrum was nearly flat with a shallow minimum at 209 nm. Upon incubation, a maximum developed at 211 nm and a minimum at 228 nm pointing to irregular coil conformations. The CD spectra observed in the presence of CLR01 suggested traces of β-sheet initially (red spectrum, Figure 4E). By 4 h, a conformational transition took place leading to a shift of the minimum to 210 nm and a decrease in its amplitude, suggesting development of disordered structures. Overall, the CD spectra indicate that EGCG and CLR01 but not Aβ(39−42) perturbed the structure of Aβ42 during the first hours of the assembly reaction and attenuated formation of the typical cross-β structure of amyloid fibrils. Similar conformational rearrangements were recorded without DMPC/DMPG vesicles present (Supplementary Figure 1).

In the next part of the study, we focused on the effect of Aβ42, the assembly modulators, and their mixtures on the membrane-bilayer structure and properties. First, we examined how addition of Aβ42 in the absence or presence of each modulator might affect membrane structure and dynamics. To address this question, we measured Förster resonance energy transfer (FRET) between a lipid-attached fluorescent donor, N-NBD-PE, and acceptor, N-Rh-PE, embedded in DMPC/DMPG vesicles. FRET has been widely used for investigating bilayer dynamics and effects of membrane-active compounds.[54,55] Addition of Aβ42 to the vesicles caused an increase of ∼30% in FRET efficiency for the duration of the experiment (Figure 5). This increase was not due to interaction

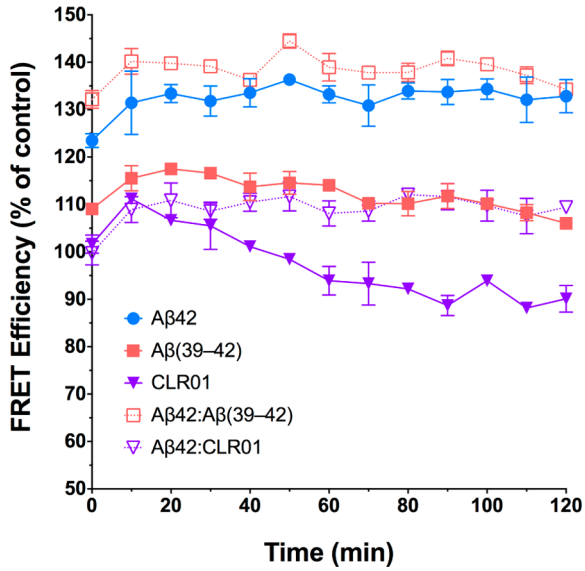

Figure 5. Effects Aβ42 in the presence or absence of Aβ(39−42) or CLR01 on energy transfer between fluorescence donor and acceptor embedded within membrane bilayers. Time-dependent changes in the FRET efficiency relative to untreated vesicles, for which the FRET efficiency was considered 100%. The concentration of Aβ42 was 30 mM, whereas concentrations of the modulators (together with the peptide or alone) were 150 μM. The data are representative of four independent experiments performed in triplicate and are presented as mean ± SEM.

of Aβ42 with the donor or acceptor themselves, because on their own, both N-NBD-PE and N-Rh-PE displayed a ∼10% decrease in fluorescence in the presence of Aβ42 (data not shown). The increase above the baseline FRET efficiency (e.g., 100%) suggested that some clustering of the fluorescence donor and acceptor molecules might have occurred, leading to more efficient energy transfer.

Figure 5 shows that addition of Aβ(39−42) had a smaller effect, increasing FRET efficiency by ∼10% relative to baseline, suggesting weaker interaction of the tetrapeptide with the

DOI: 10.1021/acschemneuro.5b00200
ACS Chem. Neurosci. 2015, 6, 1860−1869

vesicles. The FRET efficiency in the presence of the Aβ42/Aβ(39−42) mixture appeared to reflect the cumulative effect of both peptides, reaching ∼40% increase in efficiency. CLR01 caused a gradual decrease in FRET efficiency to ∼90% over the duration of the experiment (Figure 5). This effect might be ascribed to weak quenching of the fluorescence by CLR01 or to perturbation of the membrane by CLR01. Interestingly, when a mixture of CLR01 and Aβ42 was incubated with the vesicles, the FRET efficiency was ∼10% above baseline, suggesting that the interaction between Aβ42 and CLR01 negated the individual effect of the peptide (∼30% increased FRET) and the molecular tweezer (∼10% decreased FRET) on their own. The data also suggested that the decrease in FRET efficiency in the presence of CLR01 alone was due to membrane perturbation rather than quenching. FRET experiments examining the effect of EGCG were inconclusive, since EGCG had a significant quenching effect of both membrane-embedded fluorophores (Supplementary Figure 2).

To gain further insight into the impact of Aβ42 and the modulators on the membrane structure and dynamics, we used giant vesicles decorated with amphiphilic fluorescent carbon dots and examined them by confocal fluorescence microscopy (Figure 6). Carbon dots are bright, multicolored imaging agents that can be coupled readily to biological assemblies such as cells and vesicles, enabling diverse spectroscopic and microscopic visualization capabilities.[56] A recent study demonstrated that amphiphilic carbon dots could be adsorbed onto the lipid bilayers of giant unilamellar vesicles (GUV)s thereby providing a tool for visualization of membrane-associated processes and vesicle dynamics.[56]

The lipid vesicles used for the confocal fluorescence microscopy experiments in Figure 6 were PC/PG GUVs, which are substantially larger than the small unilamellar DMPC/DMPG vesicles employed in all the experiments described above, to enable microscopic visualization. However, the basic lipid types and polarity of the GUVs were maintained similar to those of the DMPC/DMPG vesicles to allow meaningful comparison with the previous experiments.

Using confocal fluorescence microscopy, we visualized for the first time the effect of Aβ42 on the membrane bilayer within minutes after addition of Aβ42 to lipid vesicles. Prior to addition of Aβ42, the vesicles exhibited a spherical morphology and uniform surface distribution of the carbon dots (Figure 6A). Addition of Aβ42 caused a dramatic time- and concentration-dependent modification of the vesicle surface organization. Addition of 5 μM Aβ42 resulted in slight distortion of the spherical vesicle shape after 10 min (the decrease of the fluorescence signal shown in the figure was recorded also in control vesicles without addition of the peptide and likely is related to bleaching of the fluorescent carbon dots over time). Addition of 15 μM Aβ42 modified the vesicle lipid arrangement more strongly giving rise to shape distortion and formation of distinct brighter and darker domains on the vesicle surface. A remarkable fluorescent "spot" was observed upon incubation of the carbon-dot-labeled vesicles with 30-μM Aβ42.

The clustering of the carbon dots into bright domains is consistent with the FRET results reported above. If similar clustering of the FRET donor and acceptor occurred, FRET efficiency would be higher in the equivalent of the bright domains and lower in the darker domains visualized by the carbon dots. The sum of the change would depended on the specific size and organization of the membrane and, as discussed above, gave rise to an overall increase of ∼30% in FRET efficiency in the presence of Aβ42.

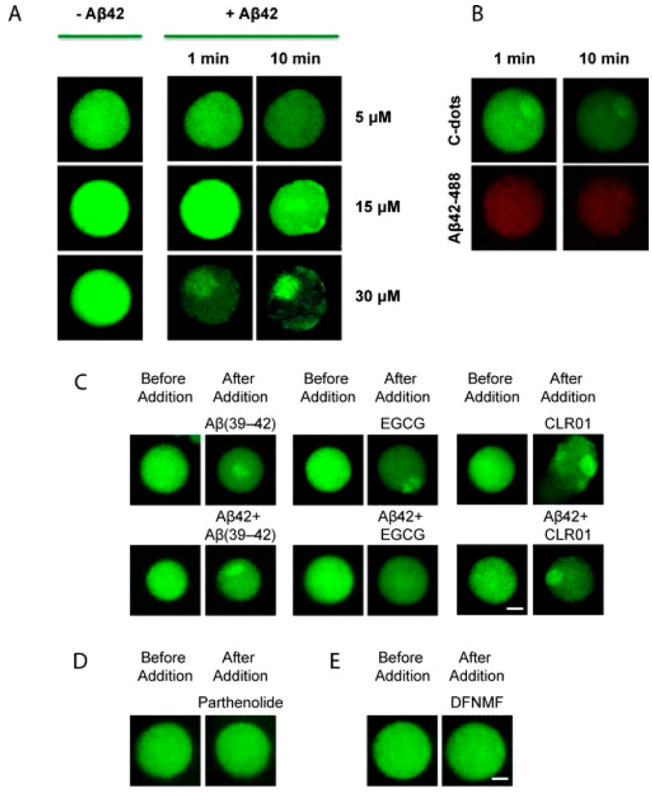

Figure 6. Interaction of Aβ42 or assembly modulators with GUVs labeled with amphiphilic carbon dots. The images show confocal microscopy images of giant unilamellar PC/PG vesicles labeled with amphiphilic fluorescent carbon dots. (A) GUVs incubated in the absence or presence of unlabeled Aβ42; (B) GUVs incubated with carbon dots; (C) GUVs incubated with carbon dots in the absence or presence of Aβ42 labeled with AlexaFluor 488 (Aβ42−488). The red color was chosen arbitrarily to distinguish the Aβ42−488 from the green carbon dots. (C) GUVs incubated in the absence or presence of Aβ42 and each of the modulators. (D) GUVs were incubated in the absence or presence of the sesquiterpene lactone parthenolide as a negative control. (E) GUVs were incubated in the absence or presence of the pentapeptide Asp-Phe-Asn-Met-Phe (DFNMF) as a negative control. In all cases, Aβ42 was added at 30 μM and the modulator at 150 μM. The images in panels C−E were taken at t = 10 min. The scale bars correspond to 5 μm.

The observed reorganization of the carbon dots upon addition of Aβ42 suggested two possible scenarios: (1) the carbon-dot reorganization reflected the changes in lipid organization within the membrane vesicles rather than direct interactions between Aβ42 and the vesicle-attached carbon dots or (2) the clustering of the carbon dots paralleled and colocalized with self-association and aggregation of Aβ42. To distinguish between these two scenarios, we incubated GUVs with carbon dots under the same conditions as in the previous experiment, but this time added Aβ42 fluorescently labeled at the N-terminal amino group by AlexaFluor 488 (Figure 6B). Examination of the images revealed that unlike the carbon dots, Aβ42 did not aggregate during the short period of interaction with the membrane and remained uniformly dispersed in the vesicle. Thus, the data support the first scenario: Aβ42 induces perturbation of the membrane and causes clustering of the carbon dots but does not coassociate with the carbon dots itself.

DOI: 10.1021/acschemneuro.5b00200
ACS Chem. Neurosci. 2015, 6, 1860−1869

Addition of each of the modulators to the PC/PG GUVs caused rearrangement of the carbon dots and in the case of EGCG and CLR01 also distortion of the vesicles. Aβ(39−42) alone induced moderate aggregation of the fluorescent carbon dots on the vesicle surface relative to Aβ42 and did not change the overall spherical morphology of the vesicle. When Aβ42 and Aβ(39−42) were coadded to the GUVs, similar vesicle surface reorganization was apparent (Figure 6C), suggesting that regardless of its own membrane activity, Aβ(39−42) offered some protection of the vesicles from the perturbation caused by Aβ42. A fluorescent "spot" was apparent, similar to the one induced by Aβ42 alone, yet the remaining surface of the vesicle did not become dark to the same extent as with Aβ42 alone (Figure 6A).

In our study design, Aβ42 and the modulators were mixed together prior to addition to the vesicles. This strategy was used to ascertain that neither Aβ42 nor the modulators exhibit (their intrinsic) membrane interactions, and accordingly the analysis would reveal whether new modes of membrane interactions occurred when the peptide and modulators interacted in solution. To validate that the effect of the compounds indeed was on each other, we also tested sequential addition, first Aβ42 and then each of the modulators or vice versa. In all the cases, the initial effect on the distribution of the carbon dots and vesicle shape persisted and was not affected by addition of the second compound (Aβ42 or any of the modulators, data not shown).

Similar to Aβ42 and Aβ(39−42), EGCG on its own also modified the distribution of the fluorescent carbon dot on the vesicle surface (Figure 6C). In addition, EGCG caused some distortion of the spherical morphology of the vesicle. The area in which the carbon dots concentrated appeared to protrude above the vesicle surface. Interestingly, when EGCG and Aβ42 were coadded to the GUVs, the vesicle morphology and surface appearance were almost identical to the control vesicles (Figure 6C), suggesting that interaction between Aβ42 and EGCG inhibited membrane disruption and reorganization by both molecules.

CLR01 had the strongest impact on the membrane among the three modulators, inducing pronounced distortion of the spherical vesicle morphology. As observed with EGCG, when CLR01 was co-incubated with Aβ42, the effect of the molecular tweezer on the vesicles was substantially less pronounced. In the presence of the Aβ42/CLR01 mixture the vesicles retained their spherical morphology and the clumping of the carbon dots into a bright patch resembled the effect of Aβ42 by itself (Figure 6C).

Because all three modulators appeared to perturb the lipid vesicles, we asked whether this was due to general nonspecific interactions with the vesicles or the carbon dots. To answer this question, we used two unrelated compounds, the anti-inflammatory sesquiterpene lactone parthenolide and the pentapeptide Asp-Phe-Asn-Met-Phe (a short fragment within the protein hormone calcitonin). Neither compound affected the distribution of the carbon dots under identical conditions (Figures 6D,E, respectively), suggesting that the observed membrane perturbation was not due to nonspecific interactions.

This study examined the relationship between the action of Aβ42 toxicity inhibitors and membrane interactions. This aspect of the antitoxic activity of compounds with therapeutic potential in amyloid diseases often has been overlooked although membrane interactions likely have important roles in mediating the toxic effects of amyloid proteins. Our data clearly show that for the three molecules examined, each representing a distinct class of antitoxic agents, incubation and association with Aβ42 substantially modulated membrane interactions.

The data confirmed that lipid vesicles promote β-sheet formation and fibril assembly by Aβ42. The distinct role of the vesicle environment was particularly apparent in the ThT fluorescence assay, which demonstrated elimination of the lag phase in the presence of vesicles, in contrast to the buffer solution (Figure 2). Similarly, the CD data showed accelerated and enhanced β-sheet formation when Aβ42 was incubated with DMPC/DMPG vesicles (Figure 4A,B). In the reverse direction, that is, the impact of Aβ42 on the membrane, FRET analysis showed an increase in FRET efficiency between lipid-embedded donor and acceptor upon addition of Aβ42 to DMPC/DMPG vesicles (Figure 5A), suggesting that Aβ42 induced clustering of the donor and acceptor. This interpretation was supported by fluorescence microscopy imaging of PC/PG GUVs labeled with amphiphilic carbon dots. Taken together, the data suggest that Aβ42 causes a substantial and rapid (within a few minutes) lipid reorganization.

Each of the three assembly modulators examined displayed its known effect in solutions containing buffer alone, confirming previous results. The presence of the lipid vesicles had a relatively minor effect on the activity of the modulators. Thus, EGCG and CLR01 prevented the ThT fluorescence increase by Aβ42 regardless of the presence of the lipid vesicles, whereas Aβ(39−42) had no effect, similar to the findings in buffer alone (Figure 2). Cryo-TEM examination of Aβ42 in the presence of vesicles revealed formation of scarce, occasional fibrils in reaction mixtures with EGCG or CLR01 (Figure 3). Similarly, the presence of lipid vesicles induced only minor changes in the CD spectra of Aβ42 in the presence of each modulator, and the kinetics of secondary-structure transition remained largely the same in each case (Figure 4). Overall, the data supported the notion that Aβ42 aggregation is facilitated by lipid vesicles but suggested that disruption of the aggregation by effective assembly modulators, such as EGCG or CLR01, is not affected by the membranes. In other words, in the push−pull competition between the membranes and the modulators, the modulators have the upper hand.

In the case of EGCG, this conclusion contradicts the observations by Engel et al., who reported that EGCG was a substantially less efficient inhibitor of amyloid formation by islet amyloid polypeptide (IAPP) in the presence of phospholipids than in simple buffer solutions.[57] The difference between our results and those of Engel et al. may simply reflect the fact that Aβ42 and IAPP are different peptides. In addition, conceivably, the differences could also be related to the distinct charge states of IAPP and Aβ42. In both studies, the vesicles had a negatively charged surface. We used a mixture of neutral DMPC and negatively charged DMPG, and Engel et al. used negatively charged dipalmitoylphosphatidylglycerol (DPPG) vesicles. In contrast to Aβ42, which has a net charge of −3 at physiologic pH, IAPP has a net charge of +3, which makes its attraction to the vesicles substantially higher than that of Aβ, providing a plausible explanation for the lower impact of EGCG on IAPP than on Aβ42 in the presence of negatively charged vesicles. If this explanation is correct, the opposite would be expected in the presence of positively charged lipid membranes, that is, EGCG would be expected to have a lower effect on Aβ42

DOI: 10.1021/acschemneuro.5b00200
ACS Chem. Neurosci. 2015, 6, 1860−1869

aggregation than on IAPP aggregation. Moreover, different lipid binding mechanisms may also play role. IAPP contains an amphipathic α-helix that can participate in binding membranes; whereas, the Aβ peptide seems to anchor into membranes more directly via the hydrophobic C-terminus.

In contrast to the unremarkable impact of the membrane vesicles on the capability of the modulators to impact Aβ42 assembly, both Aβ42 and each modulator appeared to have a substantial impact on the organization and dynamics of the lipid molecules within the vesicles. This was apparent by FRET measurements, which suggested that Aβ42 and, to a lower extent, Aβ(39−42) induced rapid clustering of the FRET donor and acceptor. In contrast, CLR01 caused slow reduction of the FRET efficiency reaching a ∼10% decrease by 2 h, suggesting perturbation of the vesicles in a manner that increased the average distance between the donor and acceptor molecules. Interestingly, this effect was reversed when CLR01 was added to the vesicles in the presence of Aβ42, even though the concentration of CLR01 was 5-times that of Aβ42.

These observations could be explained by the fact that Aβ42 may bind up to three CLR01 molecules[30] and suggest that the affinity of CLR01 for Aβ42 is substantially higher than that for the vesicles, which would be expected, because the molecular tweezer is known to bind with low micromolar affinity to lysine residues. In addition, CLR01 binds arginine residues with 5−10 times lower affinity. Upon binding of CLR01 to the lysine and arginine residues in Aβ, the charge of these residues is reversed for each lysine or arginine residue from positive (+1) to negative (ca. − 2) depending on the protonation state of the CLR01 phosphate groups,[58] increasing the net charge of Aβ42 from −3 up to −6. Thus, the complex of Aβ42 and CLR01 is expected to have a lower affinity for the membrane vesicles than Aβ42 alone. Similarly, the tendency of CLR01 to interact with the phospholipid molecules was reduced, likely due to engagement of its hydrophobic "arms" with the peptide, making them are less available for interaction with the membrane.

The fluorescence microscopy experiments utilizing carbon-dot-labeled GUVs revealed that when each of the compounds we used (including Aβ42 itself) was added individually to the vesicles it induced bilayer reorganization and in some cases caused different degrees of deformation of the globular structure of the vesicle. These membrane interactions were weaker in each case when instead of the individual compound, the mixture of each modulator with Aβ42 was added to the lipid vesicles, supporting the notion that in the interplay of the interaction of Aβ42, the lipid vesicles, and the toxicity inhibitors, the binding of the inhibitors to Aβ42 was the predominant interaction, overshadowing the interaction between Aβ42 and the membrane or the modulators and the membrane. These data suggest that in addition to their impact on Aβ42 assembly, an important mechanism by which the molecules examined here inhibit Aβ42-induced toxicity may be by reducing the interaction of Aβ42 with cell membranes. In particular, this mechanism may contribute to the inhibitory effect of Aβ(39−42), which was shown to inhibit the toxicity of Aβ42 in several cell culture tests, including cell viability and electrophysiologic assays,[18,59] without affecting Aβ42 assembly into amyloid fibrils.[34]

In summary, our study illuminates a rarely studied angle of toxicity inhibitors' activity, their effect on membrane interactions of Aβ42. The involvement of *membranes* and *membrane interactions* in Aβ toxicity in general, Aβ42 toxicity in particular, have become a widely accepted paradigm, and there have been numerous studies focusing on this aspect of amyloid biology. However, there is no consensus yet as to what exactly are the underlining links between membrane disruption and amyloid toxicity. The clear and significant modulation of membrane reorganization upon the interactions of Aβ42 and the modulators constitute an important contribution to understanding the activity of the three inhibitors and their possible therapeutic uses.

The data suggest that the interaction of Aβ42 with effective assembly modulators, EGCG and CLR01, is stronger than its interaction with membranes and that interaction with all three toxicity inhibitors partially shields Aβ42 from interacting with the membranes, contributing to the protective effect of these compounds. An open and intriguing question, which will require additional future investigation, is why the interaction of each of the compounds with the lipid vesicles, which in certain cases appeared to induce stronger perturbation than that of Aβ42, does not lead to apparent toxicity. Further high-resolution structural insights into the inhibitor−peptide−membrane system will contribute to better understanding of these issues.

METHODS

Materials. Aβ42 was purchased from AnaSpec (USA) in a lyophilized form at >95% purity. Aβ(39−42) was purchased from Peptron (South Korea) in a lyophilized form at >90% purity. L-α-Phosphatidylcholine (egg, chicken), L-α-phosphatidylglycerol (egg, chicken, sodium salt), 1,2-dimyristoyl-*sn*-glycero-3-phosphocholine (DMPC), 1,2-dimyristoyl-*sn*-glycero-3-[phospho-*rac*-(1-glycerol)] (DMPG), 1,2-dimyristoyl-*sn*-glycero-3-phosphoethanolamine-*N*-(7-nitro-2-1,3-benzoxadiazol-4-yl) (*N*-NBD-PE), and 1,2-dimyristoyl-*sn*-glycero-3-phosphoethanolamine-*N*-(lissamine rhodamine B sulfonyl) (N-Rh-PE) were purchased from Avanti Polar Lipids. Thioflavin T (ThT), 1,1,1,3,3,3-hexafluoro-2-propanol (HFIP), sodium hydrosulfite, sodium phosphate monobasic, and EGCG, >95% purity, were purchased from Sigma-Aldrich (Rehovot, Israel). CLR01 was prepared and purified as a Li^+ salt as described previously.[30,49]

Peptide and Sample Preparations. Aβ42 was dissolved in HFIP at a concentration of 1 mg/mL and stored at −20 °C until use to prevent aggregation. For each experiment, the solution was thawed, and the required amount was dried by evaporation for 6−7 h to remove the HFIP. The dried peptide sample was dissolved in 10 mM sodium phosphate, pH 7.4, at room temperature. Stock solutions of Aβ(39−42), EGCG, and CLR01 were prepared at 5 mM in deionized water and diluted into the Aβ42 solutions at the required concentration.

Thioflavin T (ThT) Fluorescence Assay. ThT fluorescence measurements were conducted at 37 °C using 96-well path cell culture plates on a Varioskan plate reader (Thermo, Finland). Measurements were made on samples containing 30 μM Aβ42 in the absence or presence of Aβ(39−42), EGCG, or CLR01 at 1:5 Aβ/inhibitor concentration ratio and in the absence or presence of lipid vesicles (final concentration 1 mM). A 192-μL aliquot of the aggregation reaction was mixed with 48 μL of 100 μM ThT in sodium phosphate, pH 7.4, at different time points. The fluorescence intensity was measured following a 10 min incubation at λ_{ex} = 440 and λ_{em} = 485 nm.

Cryogenic Transmission Electron Microscopy (Cryo-TEM). Cryo-TEM imaging of aliquots taken from the same reaction mixtures used in the ThT experiments after 12-h incubation was carried out as follows: A 3-μL droplet of the reaction mixture was deposited on a glow-discharged TEM grid (300 mesh Cu Lacey substrate grid; Ted Pella). The excess liquid was blotted with a filter paper, and the specimen was rapidly plunged into liquid ethane precooled with liquid nitrogen in a controlled environment (Leica EM GP). The vitrified samples were transferred to a cryo-specimen holder (Gatan model

DOI: 10.1021/acschemneuro.5b00200
ACS Chem. Neurosci. 2015, 6, 1860−1869

626) and examined at −181 °C using a FEI Tecnai 12 G2 TWIN TEM operated at 120 kV in low-dose mode. Grids were imaged a few micrometers under focus to increase phase contrast. The images were recorded with a Gatan charge-coupled device camera (model 794) and analyzed by Digital Micrograph software, Version 3.1.

Circular Dichroism (CD) Spectroscopy. CD spectra were recorded in the range of 190−260 nm at room temperature on a Jasco J-715 spectropolarimeter, using 1 mm quartz cuvettes. Solutions composed of 400 μL contained 50 μM Aβ42 in the absence or presence of 5-fold excess Aβ(39−42), EGCG, or CLR01 and in the absence or presence of 1 mM lipid vesicles. Spectra were recorded every 1 h for 4 h. CD signals resulting from vesicles and buffer were subtracted from the corresponding spectra.

Förster Resonance Energy Transfer (FRET). Small unilamellar vesicles (SUVs, DMPC/DMPG at 1:1 molar ratio) were prepared by dissolving the lipid components in chloroform/ethanol and drying together under vacuum, followed by dissolution in sodium phosphate, pH 7.4, and sonication of the aqueous lipid mixture at room temperature for 10 min using a Sonics vibracell VCX130 ultrasonic cell disrupter. Prior to drying, the lipid vesicles were supplemented with N-NBD-PE and N−Rh−PE at a 500:1:1 molar ratio, respectively. Aβ42 (30 μM) in the absence or presence of Aβ(39−42), EGCG, or CLR01 at 1:5 Aβ42/modulator concentration ratio was added to the vesicles (final vesicle concentration 1 mM) at $t = 0$. Fluorescence emission spectra were acquired at different time points up to 2 h (λ_{ex} = 469 nm) in the range of 490−650 nm using a Varioskan 96-well plate reader (Thermo, Finland).

To calculate the extent of FRET efficiency, the following equation was used:

$$\text{efficiency} = \frac{R_i - R_{100\%}}{R_0 - R_{100\%}} \times 100\%$$

in which R is a ratio of fluorescence emission of NBD-PE (531 nm)/rhodamine B-PE (591 nm). R_i is the ratio in the peptide/vesicle mixtures, $R_{100\%}$ was measured following the addition of 20% Triton X-100 to the vesicles, which causes complete dissolution of the vesicles, and R_0 corresponds to the ratio recorded for vesicles without any additives.

Giant Unilamellar Vesicles Labeled with Amphiphilic Carbon Dots. Amphiphilic carbon dots were prepared according to a published protocol.[56] Briefly, preparation of the carbon dots was carried out in an aqueous solution, and started with *O*,*O*′-dilauroyl tartaric acid anhydride produced through reacting L-tartaric acid with lauryl chloride. Subsequent reaction with D-glucose and hydrothermal carbonization yielded carbon dots exhibiting inner graphitic cores coated with an amphiphilic layer comprising alkyl chains and carboxylic acid moieties.[56]

Giant unilamellar vesicles (GUVs) were prepared through the rapid evaporation method.[60] Briefly, GUVs comprising egg-PC and egg-PG (1:1 mol ratio) were prepared through dissolving the lipid constituents with 1 mg of carbon quantum dots dissolved in 500 μL of chloroform through vortexing and sonication. The mixture was then transferred to a 250 mL round-bottom flask, and the aqueous phase (2.5 mL of 0.1 M sucrose, 0.1 mM KCl, 50 mM Tris solution, pH 7.4) was added carefully with a pipet and stirred gently for ∼5 min. The organic solvent was removed in a rotary evaporator under reduced pressure (final pressure 20 mbar) at room temperature. After evaporation for 4−5 min, an opalescent fluid was obtained with a volume of approximately 2.5 mL.

Confocal Fluorescence Microscopy. GUVs were imaged in the absence or presence of Aβ42, inhibitors, or their mixtures using a PerkinElmer UltraVIEW system equipped with an Axiovert-200 M (Zeiss, Germany) microscope and a Plan-Neofluar 63×/1.4 oil objective. The excitation wavelengths of 440 and 488 nm were generated by an Ar/Kr laser.

■ ASSOCIATED CONTENT

Supporting Information

The Supporting Information is available free of charge on the ACS Publications website at DOI: 10.1021/acschemneuro.5b00200.

CD data of Aβ42 and inhibitors in buffer and FRET data for EGCG (PDF)

■ AUTHOR INFORMATION

Corresponding Authors

*Raz Jelinek, Ph.D. Phone: +972-52-6839384. Fax: +972-8-6472943. E-mail: razj@bgu.ac.il.

*Gal Bitan, Ph.D. Phone: +1-310-206 2082. Fax: +1-310-206 1700. E-mail: gbitan@mednet.ucla.edu.

Author Contributions

The manuscript was written through contributions of all authors. All authors have given approval to the final version of the manuscript.

Funding

G.B. gratefully acknowledges funding from The UCLA Jim Easton Consortium for Alzheimer's Drug Discovery and Biomarker Development, the Judith & Jean Pape Adams Charitable Foundation, and Team Parkinson/Parkinson Alliance. We are also grateful to Dr. Riky Luria for help with the fluorescence measurements.

Notes

The authors declare no competing financial interest.

■ ABBREVIATIONS

AD, Alzheimer's disease; Aβ, amyloid β; EGCG, (−)-epigallocatechin-3-gallate

■ REFERENCES

(1) Huang, Y., and Mucke, L. (2012) Alzheimer mechanisms and therapeutic strategies. *Cell 148*, 1204−1222.

(2) Meissner, W. G., Frasier, M., Gasser, T., Goetz, C. G., Lozano, A., Piccini, P., Obeso, J. A., Rascol, O., Schapira, A., Voon, V., Weiner, D. M., Tison, F., and Bezard, E. (2011) Priorities in Parkinson's disease research. *Nat. Rev. Drug Discovery 10*, 377−393.

(3) Kagan, B. L., Azimov, R., and Azimova, R. (2004) Amyloid Peptide Channels. *J. Membr. Biol. 202*, 1−10.

(4) Sokolov, Y., Kozak, J. A., Kayed, R., Chanturiya, A., Glabe, C., and Hall, J. E. (2006) Soluble Amyloid Oligomers Increase Bilayer Conductance by Altering Dielectric Structure. *J. Gen. Physiol. 128*, 637−647.

(5) Lioudyno, M. I., Broccio, M., Sokolov, Y., Rasool, S., Wu, J., Alkire, M. T., Liu, V., Kozak, J. A., Dennison, P. R., Glabe, C. G., Lösche, M., and Hall, J. E. (2012) Effect of Synthetic Aβ Peptide Oligomers and Fluorinated Solvents on Kv1.3 Channel Properties and Membrane Conductance. *PLoS One 7*, e35090.

(6) Sciacca, M. F. M., Kotler, S. A., Brender, J. R., Chen, J., Lee, D.-k., and Ramamoorthy, A. (2012) Two-Step Mechanism of Membrane Disruption by Aβ through Membrane Fragmentation and Pore Formation. *Biophys. J. 103*, 702−710.

(7) Stefani, M. (2007) Generic Cell Dysfunction in Neurodegenerative Disorders: Role of Surfaces in Early Protein Misfolding, Aggregation, and Aggregate Cytotoxicity. *Neuroscientist 13*, 519−531.

(8) Kotler, S. A., Walsh, P., Brender, J. R., and Ramamoorthy, A. (2014) Differences between amyloid-[small beta] aggregation in solution and on the membrane: insights into elucidation of the mechanistic details of Alzheimer's disease. *Chem. Soc. Rev. 43*, 6692−6700.

(9) Wong, P. T., Schauerte, J. A., Wisser, K. C., Ding, H., Lee, E. L., Steel, D. G., and Gafni, A. (2009) Amyloid-β Membrane Binding and

DOI: 10.1021/acschemneuro.5b00200
ACS Chem. Neurosci. 2015, 6, 1860−1869

Permeabilization are Distinct Processes Influenced Separately by Membrane Charge and Fluidity. *J. Mol. Biol. 386*, 81−96.
(10) Terakawa, M. S., Yagi, H., Adachi, M., Lee, Y.-H., and Goto, Y. (2015) Small Liposomes Accelerate the Fibrillation of Amyloid β (1−40). *J. Biol. Chem. 290*, 815−826.
(11) Campioni, S., Mannini, B., Zampagni, M., Pensalfini, A., Parrini, C., Evangelisti, E., Relini, A., Stefani, M., Dobson, C. M., Cecchi, C., and Chiti, F. (2010) A causative link between the structure of aberrant protein oligomers and their toxicity. *Nat. Chem. Biol. 6*, 140−147.
(12) Ladiwala, A. R. A., Litt, J., Kane, R. S., Aucoin, D. S., Smith, S. O., Ranjan, S., Davis, J., Van Nostrand, W. E., and Tessier, P. M. (2012) Conformational differences between two amyloid βoligomers of similar size and dissimilar toxicity. *J. Biol. Chem. 287*, 24765−24773.
(13) Pithadia, A. S., Kochi, A., Soper, M. T., Beck, M. W., Liu, Y., Lee, S., Detoma, A. S., Ruotolo, B. T., and Lim, M. H. (2012) Reactivity of diphenylpropynone derivatives toward metal-associated amyloid-β Species. *Inorg. Chem. 51*, 12959−12967.
(14) Cheng, P. N., Liu, C., Zhao, M., Eisenberg, D., and Nowick, J. S. (2012) Amyloid β-sheet mimics that antagonize protein aggregation and reduce amyloid toxicity. *Nat. Chem. 4*, 927−933.
(15) Härd, T., and Lendel, C. (2012) Inhibition of amyloid formation. *J. Mol. Biol. 421*, 441−465.
(16) Liu, T., and Bitan, G. (2012) Modulating self-assembly of amyloidogenic proteins as a therapeutic approach for neurodegenerative diseases: strategies and mechanisms. *ChemMedChem 7*, 359−374.
(17) Gazit, E. (2002) A possible role for π-stacking in the self-assembly of amyloid fibrils. *FASEB J. 16*, 77−83.
(18) Fradinger, E. A., Monien, B. H., Urbanc, B., Lomakin, A., Tan, M., Li, H., Spring, S. M., Condron, M. M., Cruz, L., Xie, C. W., Benedek, G. B., and Bitan, G. (2008) C-terminal peptides coassemble into Aβ42 oligomers and protect neurons against Aβ42-induced neurotoxicity. *Proc. Natl. Acad. Sci. U. S. A. 105*, 14175−14180.
(19) Han, Y. S., Zheng, W. H., Bastianetto, S., Chabot, J. G., and Quirion, R. (2004) Neuroprotective effects of resveratrol against β-amyloid-induced neurotoxicity in rat hippocampal neurons: Involvement of protein kinase C. *Br. J. Pharmacol. 141*, 997−1005.
(20) Evers, F., Jeworrek, C., Tiemeyer, S., Weise, K., Sellin, D., Paulus, M., Struth, B., Tolan, M., and Winter, R. (2009) Elucidating the mechanism of lipid membrane-induced IAPP fibrillogenesis and its inhibition by the red wine compound resveratrol: a synchrotron X-ray reflectivity study. *J. Am. Chem. Soc. 131*, 9516−9521.
(21) Rezai-Zadeh, K., Arendash, G. W., Hou, H., Fernandez, F., Jensen, M., Runfeldt, M., Shytle, R. D., and Tan, J. (2008) Green tea epigallocatechin-3-gallate (EGCG) reduces β-amyloid mediated cognitive impairment and modulates tau pathology in Alzheimer transgenic mice. *Brain Res. 1214*, 177−187.
(22) Ehrnhoefer, D. E., Bieschke, J., Boeddrich, A., Herbst, M., Masino, L., Lurz, R., Engemann, S., Pastore, A., and Wanker, E. E. (2008) EGCG redirects amyloidogenic polypeptides into unstructured, off-pathway oligomers. *Nat. Struct. Mol. Biol. 15*, 558−566.
(23) Ho, L., and Pasinetti, G. M. (2010) Polyphenolic compounds for treating neurodegenerative disorders involving protein misfolding. *Expert Rev. Proteomics 7*, 579−589.
(24) Kim, D. D. S. H. L., Kim, J. Y., and Han, Y. (2012) Curcuminoids in Neurodegenerative diseases. *Recent Pat. CNS Drug Discovery 7*, 184−204.
(25) Popovych, N., Brender, J. R., Soong, R., Vivekanandan, S., Hartman, K., Basrur, V., Macdonald, P. M., and Ramamoorthy, A. (2012) Site Specific Interaction of the Polyphenol EGCG with the SEVI Amyloid Precursor Peptide PAP(248−286). *J. Phys. Chem. B 116*, 3650−3658.
(26) Huang, R., Vivekanandan, S., Brender, J. R., Abe, Y., Naito, A., and Ramamoorthy, A. (2012) NMR Characterization of Monomeric and Oligomeric Conformations of Human Calcitonin and Its Interaction with EGCG. *J. Mol. Biol. 416*, 108−120.
(27) Ladiwala, A. R. A., Lin, J. C., Bale, S. S., Marcelino-Cruz, A. M., Bhattacharya, M., Dordick, J. S., and Tessier, P. M. (2010) Resveratrol selectively remodels soluble oligomers and fibrils of amyloid Aβ into off-pathway conformers. *J. Biol. Chem. 285*, 24228−24237.
(28) Meng, F., Abedini, A., Plesner, A., Verchere, C. B., and Raleigh, D. P. (2010) The Flavanol (−)-epigallocatechin 3-gallate inhibits amyloid formation by islet amyloid polypeptide, disaggregates amyloid fibrils, and protects cultured cells against IAPP-induced toxicity. *Biochemistry 49*, 8127−8133.
(29) Pithadia, A., Brender, J. R., Fierke, C. A., and Ramamoorthy, A. (2015) Inhibition of IAPP Aggregation and Toxicity by Natural Products and Derivatives. *J. Diabetes Res.*, 907059.
(30) Sinha, S., Lopes, D. H. J., Du, Z., Pang, E. S., Shanmugam, A., Lomakin, A., Talbiersky, P., Tennstaedt, A., McDaniel, K., Bakshi, R., Kuo, P. Y., Ehrmann, M., Benedek, G. B., Loo, J. A., Klärner, F. G., Schrader, T., Wang, C., and Bitan, G. (2011) Lysine-specific molecular tweezers are broad-spectrum inhibitors of assembly and toxicity of amyloid proteins. *J. Am. Chem. Soc. 133*, 16958−16969.
(31) Attar, A., and Bitan, G. (2014) Disrupting self-assembly and toxicity of amyloidogenic protein oligomers by "molecular tweezers" - from the test tube to animal models. *Curr. Pharm. Des. 20*, 2469−2483.
(32) Bier, D., Rose, R., Bravo-Rodriguez, K., Bartel, M., Ramirez-Anguita, J. M., Dutt, S., Wilch, C., Klärner, F.-G., Sanchez-Garcia, E., Schrader, T., and Ottmann, C. (2013) Molecular tweezers modulate 14−3-3 protein−protein interactions. *Nat. Chem. 5*, 234−239.
(33) Attar, A., Chan, W. T., Klärner, F. G., Schrader, T., and Bitan, G. (2014) Safety and pharmacological characterization of the molecular tweezer CLR01 - a broad-spectrum inhibitor of amyloid proteins' toxicity. *BMC Pharmacol. Toxicol. 15*, 23.
(34) Gessel, M. M., Wu, C., Li, H., Bitan, G., Shea, J. E., and Bowers, M. T. (2012) Aβ(39−42) modulates Aβ oligomerization but not fibril formation. *Biochemistry 51*, 108−117.
(35) Li, H., Du, Z., Lopes, D. H. J., Fradinger, E. A., Wang, C., and Bitan, G. (2011) C-terminal tetrapeptides inhibit Aβ42-induced neurotoxicity primarily through specific interaction at the N-Terminus of Aβ42. *J. Med. Chem. 54*, 8451−8460.
(36) Li, H., Monien, B. H., Lomakin, A., Zemel, R., Fradinger, E. A., Tan, M., Spring, S. M., Urbanc, B., Xie, C. W., Benedek, G. B., and Bitan, G. (2010) Mechanistic investigation of the inhibition of Aβ42 assembly and neurotoxicity by Aβ42 *C*-terminal fragments. *Biochemistry 49*, 6358−6364.
(37) Palhano, F. L., Lee, J., Grimster, N. P., and Kelly, J. W. (2013) Toward the molecular mechanism(s) by which EGCG treatment remodels mature amyloid fibrils. *J. Am. Chem. Soc. 135*, 7503−7510.
(38) Attar, A., Rahimi, F., and Bitan, G. (2013) Modulators of Amyloid Protein Aggregation and Toxicity: EGCG and CLR01. *Transl. Neurosci. 4*, 385−409.
(39) Sinha, S., Du, Z., Maiti, P., Klärner, F. G., Schrader, T., Wang, C., and Bitan, G. (2012) Comparison of three amyloid assembly inhibitors: The sugar scyllo- inositol, the polyphenol epigallocatechin gallate, and the molecular tweezer CLR01. *ACS Chem. Neurosci. 3*, 451−458.
(40) Attar, A., Ripoli, C., Riccardi, E., Maiti, P., Li Puma, D. D., Liu, T., Hayes, J., Jones, M. R., Lichti-Kaiser, K., Yang, F., Gale, G. D., Tseng, C. H., Tan, M., Xie, C. W., Straudinger, J. L., Klärner, F. G., Schrader, T., Frautschy, S. A., Grassi, C., and Bitan, G. (2012) Protection of primary neurons and mouse brain from Alzheimer's pathology by molecular tweezers. *Brain 135*, 3735−3748.
(41) Doig, A. J., and Derreumaux, P. (2015) Inhibition of protein aggregation and amyloid formation by small molecules. *Curr. Opin. Struct. Biol. 30*, 50−56.
(42) Cerf, E., Sarroukh, R., Tamamizu-Kato, S., Breydo, L., Derclaye, S., Dufrêne, Y. F., Narayanaswami, V., Goormaghtigh, E., Ruysschaert, J.-M., and Raussens, V. (2009) Antiparallel β-sheet: a signature structure of the oligomeric amyloid β-peptide. *Biochem. J. 421*, 415−423.
(43) Gorbenko, G. P., and Kinnunen, P. K. J. (2006) The role of lipid-protein interactions in amyloid-type protein fibril formation. *Chem. Phys. Lipids 141*, 72−82.
(44) Chakraborty, H., and Sarkar, M. (2007) Interaction of piroxicam and meloxicam with DMPG/DMPC mixed vesicles: Anomalous partitioning behavior. *Biophys. Chem. 125*, 306−313.

DOI: 10.1021/acschemneuro.5b00200
ACS Chem. Neurosci. 2015, 6, 1860−1869

(45) Krebs, M. R. H., Bromley, E. H. C., and Donald, A. M. (2005) The binding of thioflavin-T to amyloid fibrils: Localisation and implications. *J. Struct. Biol. 149*, 30−37.
(46) Biancalana, M., and Koide, S. (2010) Molecular mechanism of Thioflavin-T binding to amyloid fibrils. *Biochim. Biophys. Acta, Proteins Proteomics 1804*, 1405−1412.
(47) Hudson, S. A., Ecroyd, H., Kee, T. W., and Carver, J. A. (2009) The thioflavin T fluorescence assay for amyloid fibril detection can be biased by the presence of exogenous compounds. *FEBS J. 276*, 5960−5972.
(48) Snitsarev, V., Young, M. N., Miller, R. M. S., and Rotella, D. P. (2013) The Spectral Properties of (−)-Epigallocatechin 3-O-Gallate (EGCG) Fluorescence in Different Solvents: Dependence on Solvent Polarity. *PLoS One 8*, e79834.
(49) Talbiersky, P., Bastkowski, F., Klärner, F. G., and Schrader, T. (2008) Molecular clip and tweezer introduce new mechanisms of enzyme inhibition. *J. Am. Chem. Soc. 130*, 9824−9828.
(50) Sani, M. A., Gehman, J. D., and Separovic, F. (2011) Lipid matrix plays a role in Abeta fibril kinetics and morphology. *FEBS Lett. 585*, 749−754.
(51) Bieschke, J., Russ, J., Friedrich, R. P., Ehrnhoefer, D. E., Wobst, H., Neugebauer, K., and Wanker, E. E. (2010) EGCG remodels mature α-synuclein and amyloid-β fibrils and reduces cellular toxicity. *Proc. Natl. Acad. Sci. U. S. A. 107*, 7710−7715.
(52) Greenfield, N. J. (1999) Applications of circular dichroism in protein and peptide analysis. *TrAC, Trends Anal. Chem. 18*, 236−244.
(53) Terzi, E., Holzemann, G., and Seelig, J. (1995) Self-association of β-amyloid peptide (1−40) in solution and binding to lipid membranes. *J. Mol. Biol. 252*, 633−642.
(54) Loura, L. M. S., De Almeida, R. F. M., and Prieto, M. (2001) Detection and characterization of membrane microheterogeneity by resonance energy transfer. *J. Fluoresc. 11*, 197−209.
(55) Gal, N., Morag, A., Kolusheva, S., Winter, R., Landau, M., and Jelinek, R. (2013) Lipid bilayers significantly modulate cross-fibrillation of two distinct amyloidogenic peptides. *J. Am. Chem. Soc. 135*, 13582−13589.
(56) Nandi, S., Malishev, R., Parambath Kootery, K., Mirsky, Y., Kolusheva, S., and Jelinek, R. (2014) Membrane analysis with amphiphilic carbon dots. *Chem. Commun. 50*, 10299−10302.
(57) Engel, M. F. M., vandenAkker, C. C., Schleeger, M., Velikov, K. P., Koenderink, G. H., and Bonn, M. (2012) The Polyphenol EGCG Inhibits Amyloid Formation Less Efficiently at Phospholipid Interfaces than in Bulk Solution. *J. Am. Chem. Soc. 134*, 14781−14788.
(58) Acharya, S., Safaie, B. M., Wongkongkathep, P., Ivanova, M. I., Attar, A., Klärner, F.-G., Schrader, T., Loo, J. A., Bitan, G., and Lapidus, L. J. (2014) Molecular Basis for Preventing α-Synuclein Aggregation by a Molecular Tweezer. *J. Biol. Chem. 289*, 10727−10737.
(59) Li, H., Zemel, R., Lopes, D. H. J., Monien, B. H., and Bitan, G. (2012) A Two-Step Strategy for Structure−Activity Relationship Studies of N-Methylated Aβ42 C-Terminal Fragments as Aβ42 Toxicity Inhibitors. *ChemMedChem 7*, 515−522.
(60) Gal, N., Malferarri, D., Kolusheva, S., Galletti, P., Tagliavini, E., and Jelinek, R. (2012) Membrane interactions of ionic liquids: Possible determinants for biological activity and toxicity. *Biochim. Biophys. Acta, Biomembr. 1818*, 2967−2974.

DOI: 10.1021/acschemneuro.5b00200
ACS Chem. Neurosci. 2015, 6, 1860−1869